




RESEARCH ARTICLE | OCTOBER 03 2024

A path-specific isentropic exponent for non-ideal compressible fluids

Jinhong Wang (汪锦弘) ; Teng Cao (曹腾)  ; Ricardo Martinez-Botas



Physics of Fluids 36, 106111 (2024)

<https://doi.org/10.1063/5.0229842>



Articles You May Be Interested In

Relationship between physical parameters of supercritical fluids and normal shock characteristics

Physics of Fluids (November 2022)

Radially symmetric non-isentropic Euler flows: Continuous blowup with positive pressure

Physics of Fluids (January 2023)

Molecular interpretation of nonclassical gas dynamics of dense vapors under the van der Waals model

Physics of Fluids (May 2006)



Physics of Fluids

Special Topic:

Kitchen Flows 2024

Guest Editors: Gerald G. Fuller, Maciej Lisicki, Arnold J.T.M. Mathijssen, Endre Joachim Mossige, Rossana Pesquino, Vivek Nagendra Prakash, Laurence Ramos

[Submit Today!](#)

A path-specific isentropic exponent for non-ideal compressible fluids

Cite as: Phys. Fluids **36**, 106111 (2024); doi: [10.1063/5.0229842](https://doi.org/10.1063/5.0229842)

Submitted: 19 July 2024 · Accepted: 13 September 2024 ·

Published Online: 3 October 2024



View Online



Export Citation



CrossMark

Jinhong Wang (汪锦弘), Teng Cao (曹腾), and Ricardo Martinez-Botas

AFFILIATIONS

Department of Mechanical Engineering, Imperial College London, South Kensington Campus, London SW7 2AZ, United Kingdom

^{a)} Author to whom correspondence should be addressed: t.cao@imperial.ac.uk

ABSTRACT

Isentropic processes are crucial in engineering as they represent idealized processes and serve as reference conditions for thermodynamic analyses. Existing methods for calculating isentropic processes in non-ideal fluids are either too slow for practical engineering applications [equation of state (EOS) approach] or inaccurate (classic modified polytropic isentrope equation: $Pv^\kappa = \text{Const.}$ where exponent κ is the isentropic expansion coefficient). This paper proposes a novel isentrope equation, $Pv^\lambda = \text{Const.}$, with a path-specific exponent λ correcting for κ variation in generic non-ideal fluid isentropic processes. The benefit of this approach is that it maintains the isentrope equation's polytropic form, so that the explicit isentropic relations can be derived, enabling straightforward and rapid calculations and a better physical understanding. Using supercritical carbon dioxide as the fluid to test the hypothesis, the proposed isentropic relations accurately calculate the stagnation state within 2% of the exact EOS calculation, whereas the classic isentropic relations have errors up to 50%. Additionally, the fitted λ function is explicit and can calculate the stagnation state approximately 15–20 times faster than the EOS approach. Moreover, the results of two other non-ideal fluids, hexamethyldisiloxane and R-143a, are included to prove the robustness and general applicability of the proposed equations. This method strikes a balance between accuracy, simplicity, and computational speed for calculating isentropic processes in non-ideal fluids, offering greatly simplified expressions for thermodynamics modeling in engineering applications such as turbomachinery reduced-order models and design optimizations.

© 2024 Author(s). All article content, except where otherwise noted, is licensed under a Creative Commons Attribution-NonCommercial-NoDerivs 4.0 International (CC BY-NC-ND) license (<https://creativecommons.org/licenses/by-nc-nd/4.0/>). <https://doi.org/10.1063/5.0229842>

I. INTRODUCTION

As a type of idealized process that is both adiabatic and reversible, isentropic processes are widely used to provide a perfect-condition reference in engineering when analyzing real thermodynamic processes. For example, isentropic efficiency is one of the most important metrics for cycle processes or turbomachines. Therefore, providing an analytical expression describing the isentropic processes is important in thermodynamics analyses.

In the literature, relations between thermodynamic properties characterizing the isentropic processes are normally referred to as isentrope equations.¹ For gases that are both thermally and calorically perfect, their isentrope equations can be analytically derived from first and second law of thermodynamics² to be in a polytropic form as Eq. (1) as follows:

$$Pv^\gamma = \text{Const.} \quad (1)$$

However, for non-ideal fluids, the ideal gas law is not applicable and the internal energy is no longer a linear function of temperature. Therefore, there are no simple isentrope equations that can be directly derived as Eq. (1). There are two major approaches available for non-ideal fluid calculations in the literature: the exact equation of state (EOS) calculation and the corrected isentrope equation.

Equations of state are equations showing the relationships of thermodynamic properties. The most typical one for perfect gas is $P = \rho RT$, which describes the relationship between pressure, density, and temperature. For non-ideal fluids, plenty EOS has been proposed in the literature such as cubic,^{3,4} viral,⁵ and Helmholtz energy-based EOS.⁶ The Helmholtz energy-based EOS is considered to be the most accurate one. Unlike ideal gas laws, which assume no interactions between molecules, the Helmholtz energy-based EOS accounts for inter-molecular forces and the resultant deviations from ideality. The thermodynamics state properties can be calculated using density ρ and temperature T as native inputs. These EOS are widely accepted in

non-ideal fluid literature to retrieve properties and are usually considered as ground truth references in thermodynamic analyses.

The expression that characterizes the isentropes using EOS would hence be simply $s = \text{Const.}$, and the specific state properties along the isentrope can be calculated using another state variable (usually enthalpy from the definition of the stagnation state). The detailed calculation procedures are included in Sec. II A. However, since entropy is not a native input of the EOS, the corresponding state needs to be calculated using reversed EOS, which involves an iterative numerical method and requires more computing times. Additionally, the complexity of EOS makes it impossible to have an explicit equation that shows how different properties vary in an isentropic process like Eq. (1), creating difficulties when modeling thermodynamic processes. Therefore, although EOS can compute properties with high accuracy, its complexity and implicit formulation make it less preferred for engineering applications that require extensive calculations and rapid responses.

The other approach to deal with non-ideal fluid isentrope behaviors is to use modified isentrope equations. Multiple alternative forms are proposed, such as Rayleigh,⁷ Callendar,⁸ and Walker⁹ equations. However, these relations were rarely used in application due to the resulting complicated form of isentropic relations (stagnation-to-static property ratio equations).¹ Therefore, in most of the non-ideal fluid literature, the polytropic form of the isentrope equation as in Eq. (1) was maintained for equation simplicity.

Due to the non-ideal fluid effects, the specific heat capacity ratio γ can no longer work as the exponent and a thermodynamic property κ , named isentropic expansion coefficient,¹⁰ becomes its substitution for non-ideal fluids. This parameter has been identified as an important thermodynamic property for non-ideal fluids and will affect flow behaviors such as normal shock,¹¹ speed of sound,¹² compressor¹³ and turbine performances.¹⁴ In the literature, its values are still treated as constants for many non-ideal fluids.¹⁵ However, for fluids near the critical point, the variation of κ is non-negligible and will cause significant errors in the isentropic relations. The detailed explanations are included in Sec. II B.

In this paper, our objective is to introduce an alternative method for isentropic process calculation in non-ideal fluids. This method seeks to balance the strengths of the EOS approach and the classic modified polytropic isentrope equation approach in terms of accuracy, simplicity, and computational speed. We present a novel isentrope equation for generic non-ideal fluids with variations in κ along the isentropes. By maintaining the simplicity of the polytropic form, we propose a new exponent, λ , to derive explicit isentropic relations, enabling straightforward and rapid calculations of non-ideal fluid isentropic processes, as well as a better physical understanding. This new exponent, λ , remains constant along a given isentropic process and is obtained through an optimization process. It is therefore a path-specific parameter, which aims to account for the κ variation in generic non-ideal fluid isentropic processes. To validate the effectiveness of our approach, we evaluate its accuracy using supercritical carbon dioxide (sCO₂) as a case study. Additional performance evaluations are also carried out using non-dimensional mass flow rates and analytical nozzle solutions.

II. THEORETICAL BACKGROUND

In this section, the two major approaches in the literature for calculating non-ideal fluid isentropic processes, namely the exact EOS

calculation and the modified polytropic isentrope equation, are explained in detail to provide a first glance at the problem.

A. Exact EOS calculation of isentropic process for non-ideal fluid

For non-ideal fluid, there are no simple explicit isentropic relations due to the deviation from perfect gas equations. Therefore, the stagnation state must be calculated using the following procedure from a given static state (any two thermal property states could work but now using pressure P and density ρ for consistency) and a given Mach number M .

1. Calculate the specific entropy of the state $s = \text{EOS}_s(P, \rho)$.
2. Calculate the specific enthalpy $h = \text{EOS}_h(P, \rho)$.
3. Calculate the speed of sound $c = \text{EOS}_c(P, \rho)$.
4. Calculate the total enthalpy $h_0 = h + 0.5(Mc)^2$.
5. Calculate the required stagnation state property using $\text{EOS}(h_0, s)$.

This is the standard non-ideal fluid isentropic relation calculation and is considered the ground truth in this study. However, as explained before, the calculation process requires multiple EOS calculations, which can be complicated and time-consuming. Moreover, the retrieved stagnation state properties are enthalpy and entropy, both of which are not native inputs of the EOS (ρ and T). Thus, the calculation of the stagnation state is much slower. Although sometimes the properties of the same state can be calculated in a single call of the EOS subroutine, three different properties (in steps 1–3) are still calculated inside the call. In addition, if lookup tables (LUT) are used, these three calculations are separate operations. The lack of an explicit equation describing the static-stagnation property ratio also makes it unfavorable in gas dynamics modeling for engineering applications.

B. Modified polytropic isentrope equation for non-ideal fluid

Alternatively, the modified isentrope equation approach can provide simple and explicit equations for isentropic processes, but will inevitably make some assumptions. The widely used polytropic isentrope equation using isentropic expansion coefficients κ is introduced and discussed in this section.

1. Isentropic expansion coefficient

Isentropic expansion coefficient or isentropic expansion exponent κ [also denoted as n_s (Ref. 16) k_{pv} (Ref. 17), and γ_{pv} (Ref. 18) in the literature] was first proposed as the “effective γ ,” which is a constant exponent for non-ideal fluid polytropic isentrope modeling.¹⁹ It is later properly defined using Eq. (2) as a fluid thermodynamic property¹⁰ and is widely used in non-ideal fluid thermodynamic models.²⁰

$$\kappa \equiv \frac{c^2 \rho}{P}. \quad (2)$$

From the definition of the speed of sound and thermodynamic relations, it can be proved (Appendix A) that κ is equivalent to a set of different forms as shown by Eq. (3).^{17,21}

$$\kappa = \frac{\rho}{P} \left(\frac{\partial P}{\partial \rho} \right)_s = -\gamma \frac{v}{P} \left(\frac{\partial P}{\partial v} \right)_T \quad (3)$$

For a thermally perfect gas, $Pv = RT$, Eq. (3) is therefore simplified to

$$\kappa = -\gamma \frac{v}{P} \left(\frac{\partial P}{\partial v} \right)_T = -\gamma \frac{v}{P} (-RTv^{-2}) = \gamma, \quad (4)$$

which indicates that the isentropic expansion coefficient κ is equal to its heat capacity ratio γ . Furthermore, if the gas is also calorically perfect (constant heat capacities), κ of such gases is a fluid-specific constant.

For non-ideal fluids, a state-specific compressibility factor $Z = Z(P, \rho)$ is introduced and the equation of state now becomes $Pv = ZRT$. Therefore, κ is no longer equal to the heat capacity ratio but becomes a state-specific property. It is important to distinguish isentropic expansion coefficient κ and heat capacity ratio γ from their definitions, which are fundamentally different.¹⁰

Research has been carried out to derive an equation of κ using different equations of states such as Redlich–Kwong–Soave²² and van der Waal's²³ EOS. In this paper, *CoolProp* library²⁴ which uses the Span–Wagner (S–W) EOS⁶ will be used to calculate the isentropic expansion coefficient values and all other properties in the non-ideal fluid calculations for accuracy.

2. Classic polytropic isentrope equation

The isentrope equation is an expression that can characterize the isentropic paths of a fluid using thermodynamic properties, such as Eq. (1). According to the state postulate,² only one property is needed to determine any thermodynamic state along each isentrope ($s = \text{Const.}$). Mathematically, it implies that a thermodynamic property along the isentrope is only a 1D function of another property [i.e., $P = P(v)$]. Therefore, the following relationship, which is derived by rearranging and integrating Eq. (3) along isentropes between two states (Appendix B), is valid for any isentropic processes by definition:

$$\ln P_1 v_1^{\kappa_1} = \ln P_2 v_2^{\kappa_2} - \int_1^2 \ln v \left(\frac{\partial \kappa}{\partial v} \right)_s dv. \quad (5)$$

If the isentropic expansion coefficient κ is constant ($\kappa_1 = \kappa_2$) along the isentrope, the integral term in Eq. (5) is zero, and the equation can be simplified as Eq. (6), which is the polytropic isentrope equation,

$$Pv^\kappa = \text{Const.} \quad (6)$$

This equation is widely used in perfect gas and non-ideal fluid thermodynamics and will be referred to as the classic polytropic isentrope equation in this paper.

Since $\kappa = \gamma$ as a fluid-specific property for perfect gases, Eq. (6) reduces to Eq. (1), which is almost globally used for perfect gas calculation.² For non-ideal fluid, although initially introduced as a constant polytropic index,¹⁹ κ is now defined as a state-specific variable and may have non-zero $\left(\frac{\partial \kappa}{\partial v} \right)_s$ values. When the variation of the isentropic expansion coefficient is small along the isentrope, Eq. (6) is a good approximation and the errors of resulting isentropic relations is negligible.^{15,25} However, significant deviation from ideal gas law is observed for fluids near the critical point.

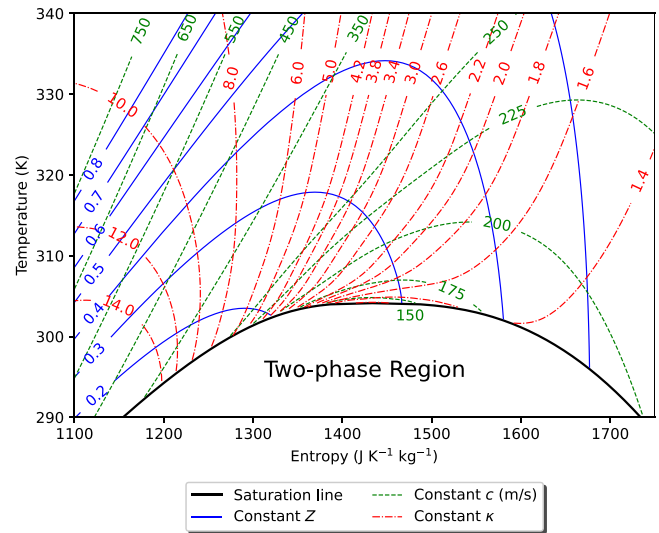


FIG. 1. T-S Diagram for CO₂ with contours of speed of sound *c*, compressibility factor *Z*, and isentropic expansion coefficient κ near the critical point.

In this paper, supercritical carbon dioxide (sCO₂) is selected as a non-ideal fluid for illustration purposes. It is a promising candidate for next-generation power cycles.²⁶ In addition, cycles closer to the critical point are shown to provide higher overall efficiency,²⁷ so it is ideal to have sCO₂ cycles that operate near the critical point. As a result, modeling sCO₂ near the critical point becomes crucial for cycle designs. Using CO₂ as an example, the solid lines in Fig. 1 show the contours of compressibility factor of CO₂ and its values are only around 0.5 near the critical point. The speed of sound (represented as dashed lines) also varies significantly and hence the variation of κ is not negligible. As a result, Eq. (6) will introduce large errors compared to Eq. (5) when calculating thermodynamic properties along the isentrope, especially with high Mach numbers when states 1 and 2 have large enthalpy differences.

3. Derived equations from classic polytropic isentrope equation

The classic polytropic isentrope equation Eq. (6) (implicitly assumes $\kappa = \text{Const.}$ along the isentrope) offers simplicity in non-ideal fluid modeling because it can provide a series of derived equations, including isentropic relations, non-dimensional mass flow rate, and the area–Mach number relation (AMR) equations.¹

a. Isentropic relations. Isentropic relations, or stagnation-to-static property ratio equations, are a set of non-dimensional equations that can calculate the ratio of stagnation and static properties. These equations are widely used in thermodynamics such as calculating stagnation states, choking mass flow rate, and analytical nozzle solution. For both perfect gases and non-ideal fluids with negligible κ variations, isentropic relations for pressure and density can be derived analytically.²⁸

Starting from the definition of stagnation state,

$$\int_h^{h_0} dh = \int_P^{P_0} v dP. \quad (7)$$

The left-hand side of the equation can be written as follows:

$$\int_h^{h_0} dh = h_0 - h = \frac{1}{2} U^2 = \frac{1}{2} M^2 c^2 = \frac{1}{2} M^2 \kappa P v. \quad (8)$$

Assuming the classic polytropic isentrope [Eq. (6)], the right-hand side of Eq. (7) can also be integrated analytically as follows:

$$\int_P^{P_0} v dP = \int_P^{P_0} v_0 \left(\frac{P_0}{P}\right)^{\frac{1}{\kappa}} dP = \frac{\kappa}{\kappa - 1} v_0 P_0 \left(1 - \left(\frac{P}{P_0}\right)^{\frac{\kappa-1}{\kappa}}\right). \quad (9)$$

Equating Eq. (8) to Eq. (9) and using the classic polytropic isentrope equation, the isentropic relations for pressure and density can be derived as Eqs. (10) and (11), respectively,

$$\frac{P_0}{P} = \left(1 + \frac{\kappa - 1}{2} M^2\right)^{\frac{\kappa}{\kappa-1}}, \quad (10)$$

$$\frac{\rho_0}{\rho} = \left(1 + \frac{\kappa - 1}{2} M^2\right)^{\frac{1}{\kappa-1}}. \quad (11)$$

These equations will be referred to as the classic isentropic relations in this paper.

It is also important to note that the isentropic relation for temperature ($\frac{T_0}{T}$) is not included because its derivation will involve additional assumptions, and hence will not be addressed in this paper.

For perfect gases, $\kappa = \gamma$ and the well-known isentropic relations can be retrieved. For non-ideal fluid with constant κ assumptions, the κ value will be calculated using the corresponding equation of state (EOS $_{\kappa}$) from the given static state. The general form of isentropic relations is still the same but now with a state-specific exponent.

For sCO₂, it was shown by Baltadjiev¹⁵ that Eqs. (10) and (11) have relative errors less than 3% when the static state is far away from the critical point. However, due to the variation of κ near the critical point, the analytical integration in Eq. (9) cannot be carried out. Therefore, the stagnation states calculated using these equations near the critical point will have significant errors.

b. Non-dimensional mass flow rate. Isentropic relations are often used to non-dimensionalize thermodynamic properties in equations such as mass flow rate. From Eqs. (10) and (11), The equation of non-dimensional mass flow rate can be derived as Eq. (12), where A is the cross-sectional area, and P_0 and ρ_0 are the stagnation state pressure and density, respectively. The derivation steps can be found in Appendix C,

$$\hat{m} = \frac{\dot{m}}{A\sqrt{P_0\rho_0}} = M\sqrt{\kappa} \left(1 + \frac{\kappa - 1}{2} M^2\right)^{-\frac{\kappa+1}{2(\kappa-1)}}. \quad (12)$$

Although Eq. (12) is normally further manipulated and simplified based on thermally and calorically perfect gas assumptions, the resulting non-dimensional mass flow rate will not be generic for all fluids with constant κ assumptions. Since this paper aims to address the non-ideal fluid effects on isentrope equations, the introduction of other assumptions will cause additional deviations and is not in our scope of discussion. Therefore, in this paper \hat{m} will be defined in a more general form as Eq. (12) to provide meaningful comparisons.

c. Area–Mach number relation (AMR) equation. Another important equation that can be derived from the classic polytropic isentrope

equation and the resulting isentropic relations is the area–Mach number relation (AMR) equation.

If the nozzle flow is isentropic, the stagnation state will be the same at all locations and hence Eq. (13) can be derived from the mass conservation ($\dot{m}_1 = \dot{m}_2$) and Eq. (12),

$$\frac{A_1}{A_2} = \frac{M_2}{M_1} \sqrt{\frac{\kappa_2}{\kappa_1}} \left(1 + \frac{\kappa_2 - 1}{2} M_2^2\right)^{-\frac{\kappa_2+1}{2(\kappa_2-1)}} \left(1 + \frac{\kappa_1 - 1}{2} M_1^2\right)^{\frac{\kappa_1+1}{2(\kappa_1-1)}}. \quad (13)$$

This equation is normally used to calculate analytical solutions for isentropic nozzles with area variations, and hence aid the nozzle designs in experiments and industry.

d. Calculation procedure using classic polytropic isentrope equation. With the help of explicit equations derived in Sec. II B 3a, the calculation procedure is greatly simplified:

1. Calculate the isentropic expansion coefficient $\kappa = \text{EOS}_{\kappa}(P, \rho)$.
2. Calculate the stagnation pressure P_0 and density ρ_0 using Eqs. (10) and (11).
3. Calculate the required stagnation state property using $\text{EOS}(P_0, \rho_0)$.

Compared to the analytical calculation procedure in Sec. II A, the modified isentrope equation approach only calculates the EOS once for the value of κ . In addition, one of the retrieved stagnation state properties is density, which is a native input of the EOS. Therefore, the calculation speed can be increased significantly compared to the EOS calculation.

C. Research gap

In summary, a dilemma exists in the literature regarding the calculation of isentropic processes for non-ideal fluids. While the equation of state (EOS) approach provides accurate property calculations along the isentrope, its complexity and implicit nature considerably slow down related applications such as low-order thermodynamic modeling and design optimizations. Furthermore, maintaining the classical form of the isentrope equation approach offers explicit analytical expressions and is much faster for isentropic process calculations. However, this approach did not consider the variation of κ along the isentrope and the direct application of this method will introduce huge errors when $\left(\frac{\partial \kappa}{\partial v}\right)_s$ is not trivial. Therefore, a new approach is proposed here that strikes a balance between accuracy, equation simplicity, and computational speed, which is needed for calculating isentropic processes in non-ideal fluids.

III. METHODS

A. New approach for non-ideal fluid isentropic process calculation

1. New polytropic isentrope equation with path-specific exponent

For the new model for non-ideal fluids, the polytropic form of the isentrope equation is retained due to its simplicity. In this paper, we propose a new exponent of λ that is sufficiently accurate to characterize the given isentropic process; hence, the new isentrope equation is given by Eq. (14),

$$Pv^\lambda = \text{Const.} \tag{14}$$

The new exponent is considered to be a constant for the given isentropic process (characterized by a static state and a Mach number). This means that the exponent in Eq. (14) is now a path- or process-specific parameter instead of a state-specific parameter as in Eq. (6).

By retaining the polytropic form of the isentrope equation as Eq. (6), the value of λ will be equal to γ for perfect gas and κ for fluid with negligible κ variations, respectively. For regions with large isentropic expansion coefficient variation, λ will not be equal to κ due to the integral term in Eq. (5) and needs to be found for each isentropic process. The value of λ is obtained through an optimization process to minimize a defined equivalent error, which will be introduced in Sec. III B 1.

2. Derived equations from new polytropic isentrope equation

a. New isentropic relations. By maintaining the polytropic form in the new isentrope equation, the derivation of the isentropic relation with the new exponent is similar to in Sec. II B 3. The isentropic expansion coefficient κ has two different origins in the previous derivation: 1. the speed of sound calculation, and 2. the polytropic index of isentrope equation Eq. (6). The proposed equations now distinguish these two different origins and use the new path-specific exponent λ as the polytropic index of isentrope equation Eq. (14).

Starting from Eq. (7), the left-hand side of the equation remains the same as Eq. (8) and the right-hand side of the equation is now with the new exponent λ instead,

$$\int_P^{P_0} v \, dP = \int_P^{P_0} v_0 \left(\frac{P_0}{P}\right)^{\frac{1}{\lambda}} dP = \frac{\lambda}{\lambda - 1} v_0 P_0 \left(1 - \left(\frac{P}{P_0}\right)^{\frac{\lambda - 1}{\lambda}}\right). \tag{15}$$

Since we assume λ to be a constant for each isentropic process, the integral in Eq. (15) is exact. The new isentropic relation using the proposed model can hence be derived as Eqs. (16) and (17) for pressure and density, respectively,

$$\frac{P_0}{P} = \left(1 + \frac{\kappa \lambda - 1}{\lambda} M^2\right)^{\frac{\lambda}{\lambda - 1}}, \tag{16}$$

$$\frac{\rho_0}{\rho} = \left(1 + \frac{\kappa \lambda - 1}{\lambda} M^2\right)^{\frac{1}{\lambda - 1}}. \tag{17}$$

Comparing Eqs. (16)–(17) with (10)–(11), the new isentropic relations substitutes κ in the classic isentropic relation with the new exponent λ and has an additional term of $\frac{\kappa}{\lambda}$. The equation simplicity is retained because Eq. (14) is in polytropic form. The κ term in Eq. (16)–(17) originated from the speed of sound and hence needs to be calculated using EOS_κ like in Sec. II B 3.

For perfect gases and non-ideal fluids with constant isentropic expansion coefficient, the $\frac{\kappa}{\lambda}$ term is equal to unity and Eq. (16)–(17) will fall back to the classic isentropic relations as Eq. (10)–(11).

b. New Non-dimensional Mass Flow Rate. From the new isentropic relations derived in Sec. III A 2, the consequent non-dimensional mass flow rate \hat{m} can be derived as follows:

$$\hat{m} = \frac{\dot{m}}{A\sqrt{P_0\rho_0}} = M\sqrt{\kappa} \left(1 + \frac{\kappa \lambda - 1}{\lambda} M^2\right)^{-\frac{\lambda + 1}{2(\lambda - 1)}}. \tag{18}$$

c. New area-Mach number relation (AMR) equation. The area-Mach number relation equation can also be calculated as Eq. (19) as follows:

$$\frac{A_1}{A_2} = \frac{M_2}{M_1} \sqrt{\frac{\kappa_2}{\kappa_1}} \left(1 + \frac{\kappa_2 \lambda_2 - 1}{\lambda_2} M_2^2\right)^{-\frac{\lambda_2 + 1}{2(\lambda_2 - 1)}} \left(1 + \frac{\kappa_1 \lambda_1 - 1}{\lambda_1} M_1^2\right)^{\frac{\lambda_1 + 1}{2(\lambda_1 - 1)}}. \tag{19}$$

Just like the new isentropic relations and non-dimensional mass flow rate equation, it is in a similar form as Eq. (13) but with κ and λ at the same time due to their different origin in the derivation. In addition, since the AMR involves two static states with the same stagnation state, Eq. (19) is a combination of two sets of isentropic relations with two path-specific exponents λ_1 and λ_2 .

3. Calculation procedure using new isentrope equation

With the proposed isentropic relations (Sec. III A 2 a), the calculation of stagnation state in Sec. II A can be greatly simplified. Starting again from the static state (P, ρ) and Mach number M :

1. Calculate the isentropic expansion coefficient $\kappa = \text{EOS}_\kappa(P, \rho)$.
2. Calculate the path specific exponent λ for the given isentropic process.
3. Calculate the stagnation pressure P_0 and density ρ_0 using Eqs. (16) and (17).
4. Calculate the required stagnation state property using $\text{EOS}(P_0, \rho_0)$.

Compared to the classic isentrope equation method, the only additional step is to calculate λ . If λ can be calculated explicitly in step 2, the computation speed is still faster compared to the EOS approach. In this paper a polynomial of $\lambda(P, \rho, M)$ is fitted as a proof of concept.

B. Model validation

The proposed method is then evaluated for its accuracy when calculating the non-ideal fluid isentropic processes and its performance in applications.

1. Error quantification metric

To examine the accuracy of the isentrope equations, an error quantification metric needs to be selected. Since the isentrope equations are given as the relationship between pressure and density [Eqs. (1), (6), and (14)], stagnation pressure P_0 and density ρ_0 are the properties that are directly calculated from the isentropic relations to determine the stagnation state. Errors of other state properties originate from errors in P_0 and ρ_0 . Therefore, an effective error based on P_0 and ρ_0 is introduced and used in this paper.

For a given static state and Mach number, the exact stagnation pressure $P_{0-\text{EOS}}$ and density $\rho_{0-\text{EOS}}$ can be calculated using the EOS approach (Sec. II A) and will be treated as ground truth for error analysis. The modeled stagnation pressure $P_{0-\text{model}}$ and density $\rho_{0-\text{model}}$ can be calculated using different isentropic relations [Eqs. (10) and (11) or

(16) and (17)], accordingly. The relative errors in P_0 and ρ_0 can hence be calculated using Eq. (20) as follows:

$$\text{Error}_{P_0} = \left| \frac{P_{0-\text{EOS}} - P_{0-\text{model}}}{P_{0-\text{EOS}}} \right|, \quad \text{Error}_{\rho_0} = \left| \frac{\rho_{0-\text{EOS}} - \rho_{0-\text{model}}}{\rho_{0-\text{EOS}}} \right|. \quad (20)$$

Finally, the effective errors introduced by the modeled isentropic equation can be quantified using Eq. (21), which calculates the root mean square (RMS) of the relative errors in P_0 and ρ_0 . The RMS is used to penalize the large errors more heavily,

$$\text{RMSE} = \sqrt{\frac{\text{Error}_{P_0}^2 + \text{Error}_{\rho_0}^2}{2}}. \quad (21)$$

This effective error is therefore a synthetic metric and its numerical value can be interpreted as the relative error in the calculated stagnation state from the actual state calculated using steps in Sec. II A.

2. Non-ideal fluid selection and study range setup

The proposed polytropic isentropic equation is developed for generic non-ideal fluids. Supercritical carbon dioxide (sCO₂) was chosen as a non-ideal compressible fluid example with κ variation due to its increasing interest in power generation. Power cycles with sCO₂ operate near the critical point to maximize the efficiencies and may suffer from non-ideal fluid isentropic behaviors.

The investigation range is given in temperature T and specific entropy s , and is selected based on typical sCO₂ compressor operating conditions, with $305 \leq T \leq 320$ K and $1300 \leq s \leq 1550$ JK⁻¹kg⁻¹. This is also a range close to the critical point and hence with a large variation of thermal properties. The Mach number range is selected to be below 1.5 and the resulting maximum stagnation temperature is around 420 K. All non-ideal fluid state properties are calculated using *CoolProp* library,²⁴ which uses the state-of-art Span–Wagner (S–W) EOS.⁶

3. Exponent optimization and regression

The values of path-specific exponent λ are then optimized and fitted using *scipy.optimize* library.²⁹ For each isentropic process within the studied range, the effective error defined as Eq. (21) is minimized. The optimized λ is then fitted for an explicit equation, enabling faster calculations. A third-order polynomial regression using Eq. (22) is

carried out in this paper as a simple example but any sensible fitting method may be applied,

$$\lambda(P, \rho, M) = \sum_{i=0}^3 \sum_{j=0}^{3-i} \sum_{k=0}^{3-i-j} a_{ijk} P^i \rho^j M^k. \quad (22)$$

In this paper, the inputs of the λ regression equation are static pressure P , static density ρ , and Mach number M . Pressure and density are selected because the isentropic relations are given for $\frac{P_0}{P}$ and $\frac{\rho_0}{\rho}$, but any combination of two thermodynamic properties can potentially work depending on different applications (different known properties).

4. Further performance evaluation

Apart from the effective error defined using Eq. (21), additional validation methods can be used to further examine the accuracy of the proposed isentropic equation. A summary is included in Table I.

a. Non-dimensional mass flow rate. The non-dimensional mass flow rate (\hat{m}), which is commonly used to evaluate the choking mass flow rate, can be calculated analytically. Four different calculations are carried out for comparison as shown in Table I.

1. Non-ideal fluid EOS calculation calculates the static states from specified stagnation state and Mach number iteratively using S–W EOS. For the given stagnation state, the total enthalpy h_0 and entropy s can be retrieved. Starting with an approximated speed of sound c , the static state can be determined using $\text{EOS}(h_0 - 0.5(Mc)^2, s)$ and the c can be updated until convergence. The value of non-dimensional mass flow rate can hence be calculated directly using $\hat{m} = \frac{\rho M c}{\sqrt{P_0 \rho_0}}$. The results from the EOS calculation are used as the ground truth for the analysis.
2. For perfect gas CO₂ calculation, κ is a constant hence Eq. (12) is explicit and can be calculated directly.
3. For classic polytropic isentropic calculations the state-specific isentropic expansion coefficient κ must be iterated for the static state. Starting with an approximated κ , the static pressure P and density ρ can be calculated using Eqs. (10) and (11), respectively, for the given stagnation state $\{P_0, \rho_0\}$ with Mach number M . The value of κ can hence be updated using $\text{EOS}_\kappa(P, \rho)$ until convergence and \hat{m} can be calculated using Eq. (12).
4. For calculations with the new polytropic isentropic equation, both state-specific κ and path-specific λ need to be iterated.

TABLE I. Summary of calculation methods for comparison.

Calculation method	Isentropic equation	Value of exponent	Non-dimensional mass-flow rate equation	Analytical nozzle solution
Non-ideal fluid EOS	$s = \text{Const.}$	N.A.	$\hat{m} = \frac{\rho M c}{\sqrt{P_0 \rho_0}}$ ^a	Mass continuity
Perfect gas CO ₂	Eq. (6)	$\kappa = 1.28$	Eq. (12)	Eq. (13)
Classic polytropic isentropic	Eq. (6)	$\kappa = \text{EOS}_\kappa(P, \rho)$	Eq. (12) ^b	Eq. (13)
New polytropic isentropic	Eq. (14)	$\lambda = \lambda(P, \rho, M)$	Eq. (18) ^c	Eq. (19)

^aConverging $c = \text{EOS}_c(h_0 - 0.5(Mc)^2, s)$.

^bConverging $\kappa = \text{EOS}_\kappa(P(P_0, M, \kappa), \rho(P_0, M, \kappa))$.

^cConverging $\kappa = \text{EOS}_\kappa(P(P_0, M, \kappa, \lambda), \rho(P_0, M, \kappa, \lambda))$ and $\lambda = \lambda(P(P_0, M, \kappa, \lambda), \rho(P_0, M, \kappa, \lambda), M)$.

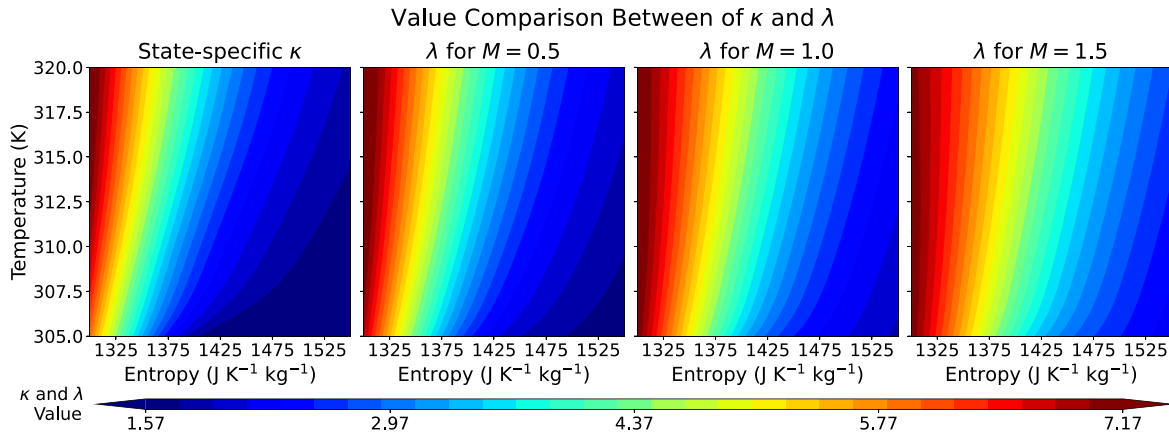


FIG. 2. Contours of isentropic expansion coefficient κ and optimized path-specific exponent λ .

From guessed κ and λ , the static pressure P and density ρ can be calculated from given P_0 , ρ_0 and M using Eqs. (16) and (17), respectively. The values of κ and λ can therefore be updated using $\text{EOS}_\kappa(P, \rho)$ and $\lambda(P, \rho, M)$ until convergence. Equation (18) is then used to calculate \hat{m} .

The stagnation temperature is set to be 350 K so that the corresponding sonic states are within our specified range in Sec. III B 2. A Mach number range from 0.75 to 1.1 was used for the calculation to show the \hat{m} variation close to the sonic state (choking condition). Three cases with different entropy levels (1325, 1425, and 1525 $\text{J K}^{-1} \text{kg}^{-1}$) were calculated for comparison.

b. Analytical solution for isentropic de Laval nozzles. Finally, a set of analytical nozzle calculations were carried out to further examine the accuracy of the proposed isentrope equation with path-specific exponent λ . A de Laval nozzle was used for all calculation cases and its geometry is included in Table V in Appendix E. The nozzle geometry is modified based on the literature³⁰ to ensure that the flow within the nozzle remains fully supersonic at the given stagnation states. The stagnation temperature for the nozzle cases is set to be 420 K and three different entropy cases ($s = 1325, 1425, \text{ and } 1525 \text{ J K}^{-1} \text{kg}^{-1}$) were set up for comparison. In addition, the nozzles are assumed to be choked and fully expanded without shock waves so that the flow is isentropic.

As explained in Sec. III B 4 a, four calculations were carried out for comparison: non-ideal fluid calculation with EOS, perfect gas CO_2 , classic and new isentrope equation, as shown by Table I. Since the flow is choked and fully expanded to the supersonic region, the sonic states at the throat can be calculated using P_0 , ρ_0 with $M = 1$. The calculated sonic state can therefore be used as the reference state [state 1 in AMR equations Eqs. (13) and (19)] to solve for other locations (state 2 in the equations). The corresponding AMR equations are used for different calculation methods and the iterative procedures to retrieve exponent values and the static states are similar to Sec. III B 4 a.

IV. RESULTS

A. Comparison between κ and λ values

Since the proposed isentrope equation Eq. (14) is in the same form as the classic polytropic isentrope equation Eq. (6), the values of

isentropic expansion coefficient κ and optimized path-specific exponent λ can be directly compared for some insights in the non-ideal fluid isentrope behaviors.

The contours for the κ and λ in our investigation static state range are plotted on T-S diagrams as shown by Fig. 2. Since κ is a state-specific thermodynamic property by definition, it is only plotted in the first subplot. As explained in Sec. III A 1, the proposed exponent λ is a path-specific value and will vary depending on the Mach number. Therefore, the contours of λ are shown for three featuring Mach number, 0.5, 1.0 and 1.5 on second to fourth subplots in Fig. 2.

In general, the value of optimal λ increases with the Mach number and greater differences between κ and λ are reported for higher M , which is as expected. The kinetic energy of the flow is higher with a large M , resulting in a greater enthalpy and temperature difference between the static and stagnation states. As a result, the variation of κ along the isentrope is greater so that the corrected isentrope equation Eq. (14) will have a more significant deviation from Eq. (6), which is reflected by the numerical difference in the values of λ and κ .

The most significant difference between κ and λ is observed when the static temperature is close to the critical temperature ($T < 307 \text{ K}$). This is again due to the large variation of κ along the isentrope. As shown by Fig. 1, the isolines of the isentropic expansion coefficient are densely distributed near the critical point. On the isentrope of $s = 1425 \text{ J K}^{-1} \text{kg}^{-1}$, a small increase in temperature from 305 to 307 K will result in an increase in κ from 1.53 to 2.06. Therefore, even with a low Mach number, the isentropic process from the static to stagnation state will have significant κ variations, leading to the larger integral term in Eq. (5) and hence significant differences between λ and κ .

B. Error comparisons between classic and new isentrope equations

The effective stagnation state errors are plotted on T-S diagrams in Fig. 3 for both classic and new isentrope equation calculations. Each point on the T-S diagram (100 data points in each dimension) represents a given static state $\{T, s\}$ and the color contours represent the value of effective errors defined as Eq. (21). On different rows in Fig. 3, results for three featuring Mach numbers (0.5, 1.0, and 1.5) are plotted to show the Mach number effect. For each given static state and Mach

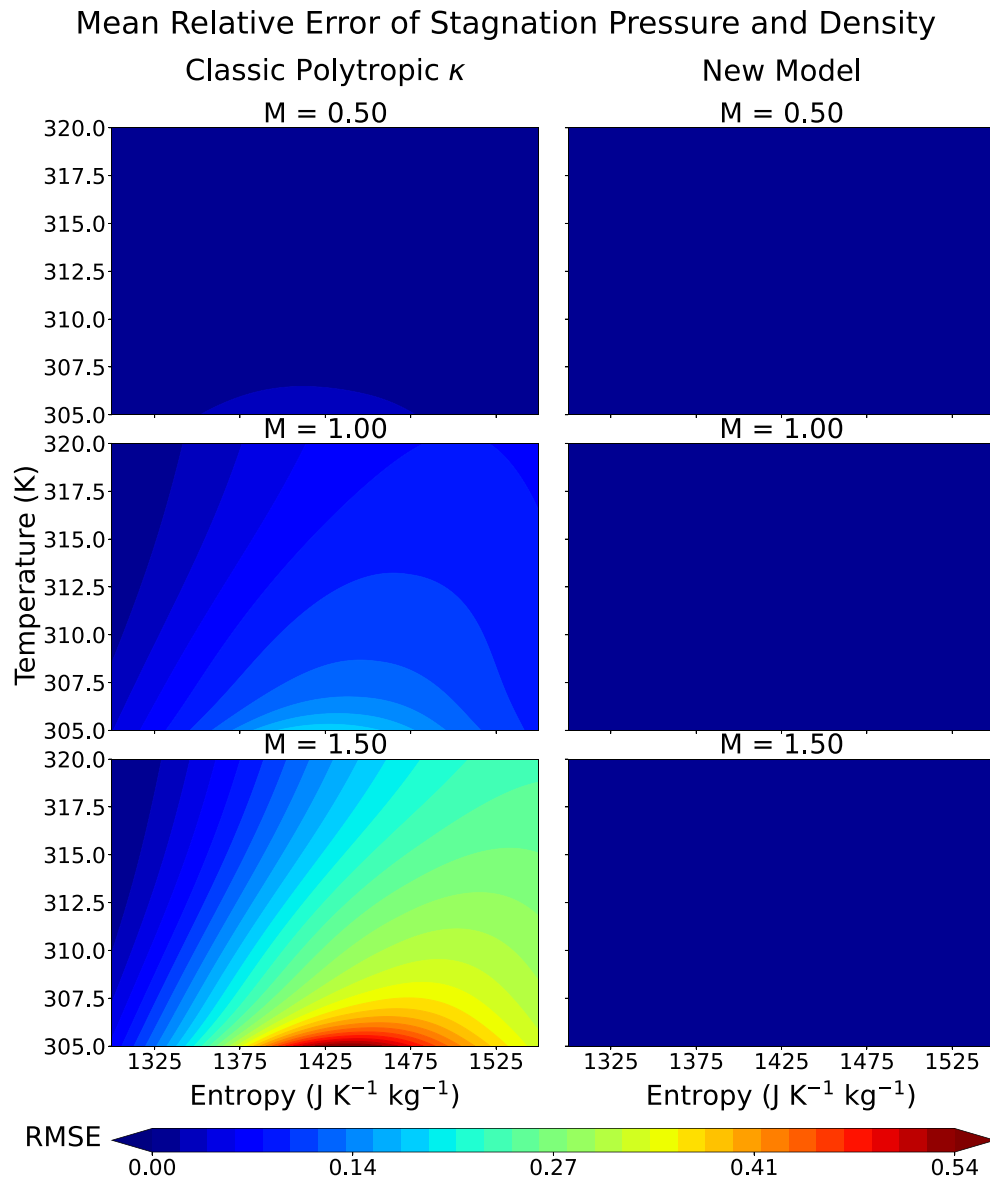


FIG. 3. Effective error comparison between the classic polytropic isentrop equation (6) (left column) and the new isentrop equation (14) with optimized λ (right column) at different Mach number for $s\text{CO}_2$.

number, the stagnation pressure and density can be calculated using different equations. Assuming the classic polytropic isentrop equation, Eqs. (10) and (11) are used to calculate P_0 and ρ_0 . The effective error (using the EOS calculation results as the ground truth) is then calculated and the results are shown by the graphs on the left column. Similarly, Eqs. (16) and (17) are used to calculate P_0 and ρ_0 for new isentrop equation and the resulting error is plotted on the right column graphs. The optimized values of λ are used for the calculation to show the model accuracy.

For the results using the classic isentrop equation, the errors of the evaluated stagnation state increase with Mach number and are at

maximum near the critical point. As explained in Sec. IV A, for higher Mach numbers or when the static states are near the critical point, the κ variation for an isentropic process from static to stagnation state is significant so Eq. (6) is not applicable. As a result, the consequent classic isentropic relations [Eqs. (10) and (11)] will have huge errors when calculating the stagnation properties. The relative error in the stagnation state is up to 50% when compared to the EOS result.

By contrast, it is obvious from Fig. 3 that the isentropic relations that are derived from the new isentrop equation Eq. (14) with optimized path-specific exponent λ has much lower error when evaluating the stagnation state. The maximum effective error for the new

isentropes is only 1.6% when compared with the EOS calculated state, even with higher Mach numbers and near the critical point.

For a better understanding of the model behavior, the effective error of the new isentropes is shown again on the left-column graphs in Fig. 4 but with different color scales. As expected, the error is higher for larger Mach numbers just like the classic polytropic isentropes. In addition, a trend of increasing error with specific entropy is observed on graphs with $M = 1.0$ and 1.5 . This is due to the small variation of isentropic expansion coefficient κ in the low entropy region within our range of study. In Fig. 1, the isolines for κ

are almost vertical when s is around $1325 \text{ J K}^{-1} \text{ kg}^{-1}$ while the density variation along isentropes remains unchanged, indicating a lower value of $(\frac{\partial \kappa}{\partial v})_s$ compared to a calculation with higher s .

In addition, to prove the robustness and general applicability of the proposed model, two additional non-ideal fluids, hexamethyldisiloxane (MM) and R-143a. The investigation range and results are summarized in Appendix D. For both of the fluids, the proposed model is at least an order of magnitude more accurate when compared to the classic polytropic isentropes, indicating that the proposed framework works well for different non-ideal fluids.

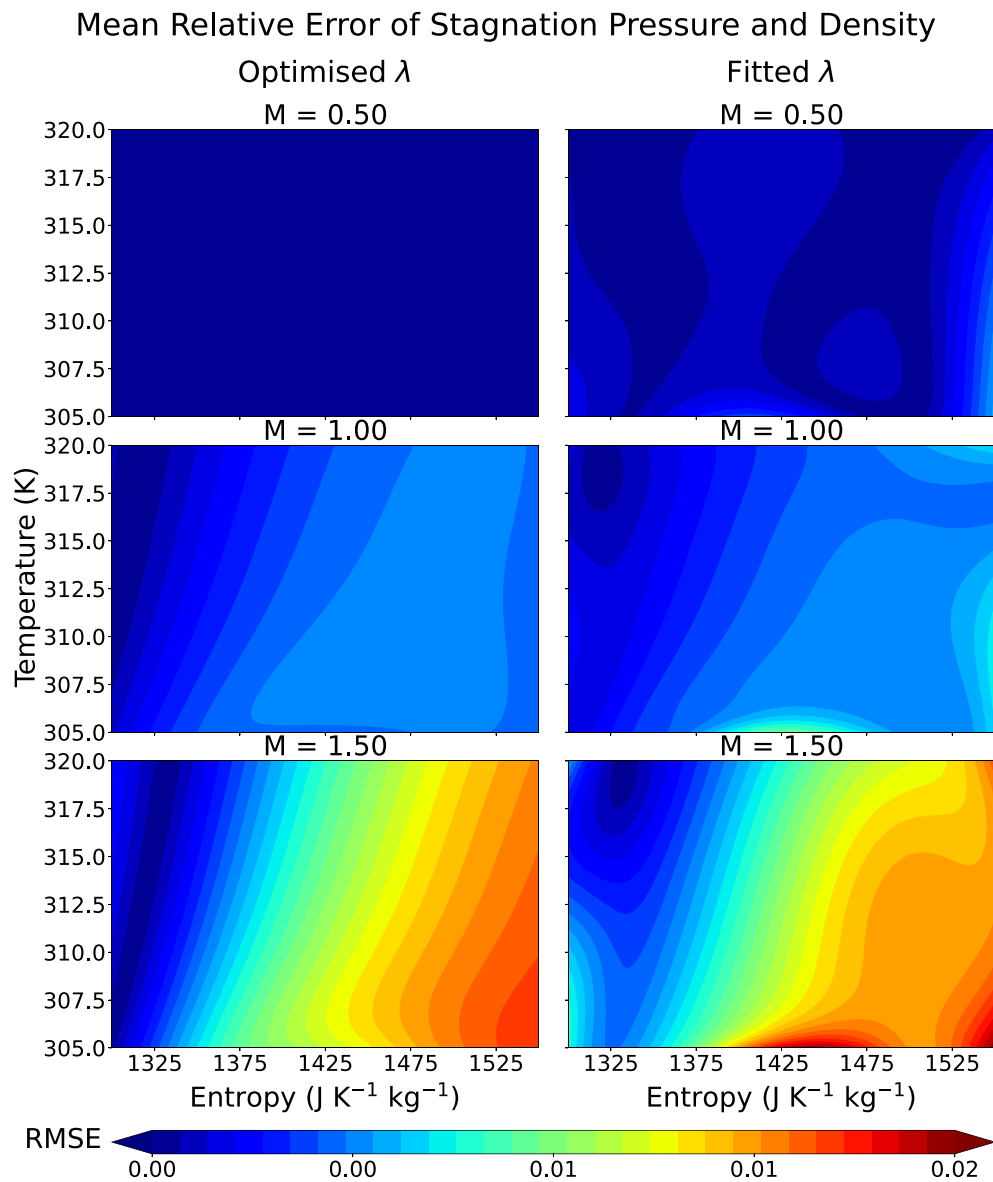


FIG. 4. Effective error comparison between the classic polytropic isentropes equation (6) with optimized path-specific λ (left column) and λ calculated using the fitted polynomial equation (22) (right column) at different Mach number.

11 October 2024 09:22:31

TABLE II. Coefficients of fitted polynomial equation (22) for $\lambda(P, \rho, M)$.

Coef.	Values	Coef.	Values	Coef.	Values	Coef.	Values
a_{000}	$3.263\ 419\ 18 \times 10^{00}$	a_{020}	$5.278\ 823\ 58 \times 10^{-05}$	a_{300}	$-6.428\ 151\ 40 \times 10^{-22}$	a_{120}	$-8.152\ 851\ 71 \times 10^{-12}$
a_{100}	$2.291\ 879\ 44 \times 10^{-06}$	a_{002}	$2.203\ 895\ 24 \times 10^{-01}$	a_{030}	$5.455\ 576\ 89 \times 10^{-08}$	a_{021}	$-2.313\ 940\ 48 \times 10^{-05}$
a_{010}	$-5.699\ 610\ 97 \times 10^{-02}$	a_{110}	$2.120\ 077\ 95 \times 10^{-09}$	a_{003}	$-1.672\ 507\ 42 \times 10^{-02}$	a_{102}	$1.038\ 111\ 96 \times 10^{-07}$
a_{001}	$-3.897\ 060\ 01 \times 10^{00}$	a_{101}	$-6.186\ 816\ 55 \times 10^{-07}$	a_{210}	$3.282\ 067\ 24 \times 10^{-16}$	a_{012}	$-2.655\ 786\ 31 \times 10^{-03}$
a_{200}	$-2.134\ 554\ 32 \times 10^{-13}$	a_{011}	$3.136\ 769\ 24 \times 10^{-02}$	a_{201}	$2.033\ 914\ 43 \times 10^{-14}$	a_{111}	$-1.545\ 199\ 56 \times 10^{-10}$

C. Regression for λ

As explained in Sec. III B 3, a third-order polynomial equation $\lambda(P, \rho, M)$ is fitted for faster calculations. The coefficients of the polynomial are shown in Table II and with coefficient names defined as Eq. (22).

The fitted polynomial has a R^2 value of 0.999187 and the effective stagnation state error comparison between the optimal and fitted λ is shown in Fig. 4. The graphs are T-S diagrams just like Fig. 3 and graphs on different rows are for three different Mach numbers. The left column graphs are now the error using Eqs. (16) and (17) with optimized λ (the same as the right column graphs in Fig. 3 but with different color scales). The effective error calculated using the same equations but now using fitted polynomial $\lambda(P, \rho, M)$ calculated exponents are plotted on the right column graphs. Compared to the calculation with optimized λ , calculations using fitted λ have greater errors when the static state is near the critical point or has a higher value of entropy. This is expected because these are the conditions when the variation of κ along isentrope is most significant. Nevertheless, the maximum effective relevant error is below 2% from the actual stagnation state calculated using EOS, which is negligible compared to the errors from the classic polytropic isentrope equation with κ as shown in Fig. 3.

To extend the applicable range of this method, we can apply the same method at different TS ranges. Since regions near the critical point suffer most from the effect of κ variation along the isentrope and this section has shown that the proposed model works well in this region, the proposed model with path-specific exponent λ will work better in regions away from the critical point and have smaller errors when evaluating stagnation states.

In addition, the fitted polynomial accelerated the stagnation state calculation process significantly due to its simplicity and explicit nature. In order to provide a fair calculation speed comparison, the static state is specified using pressure P and density ρ . For the stagnation state, we are calculating two native inputs (T_0 and ρ_0) as the final output. The calculation procedure strictly follows Secs. II A and III A 3. CoolProp high-level interface was used to calculate non-ideal fluid properties. In the same code environment, 1000 calculations of stagnation state using the EOS approach take 2.751 s and the proposed model only takes 0.144 s. The calculation of the stagnation state using the proposed equation is around 15–20 times faster than the calculation using the EOS approach.

D. Further Performance Evaluations

1. Non-dimensional mass flow rate

The calculated non-dimensional mass flow rate (\hat{m}) using different methods as explained in Sec. III B 4 were plotted on the left,

middle, and right graph in Fig. 5 for $s = 1325, 1425,$ and $1525 \text{ JK}^{-1}\text{kg}^{-1}$, respectively.

The perfect gas CO_2 calculations (dotted lines) have the most significant deviation from the EOS calculation (solid lines) in Fig. 5. This is due to the difference in the value of κ . In perfect gas literature for CO_2 , a typical value of 1.28 was used but its value near the critical point is higher and keeps increasing with reducing s as shown by Fig. 1. This also explains the increasing deviation between perfect gas CO_2 and the EOS calculations with decreasing specific entropy s .

As for the non-dimensional mass flow rate calculated using state-specific κ (dashed lines), the error is smaller compared to perfect gas CO_2 results but has a much more serious issue. In theory, the non-dimensional mass flow rate is at its maximum with $M = 1$, which is the choking condition of the flow. However, the classic polytropic isentrope equation predicted the maximum \hat{m} when M is below 8.5. Therefore, the classic polytropic isentrope equation will underestimate the choking mass flow rate at $M = 1$ as shown by Fig. 5. This will cause significant problems for low-order model predictions such as turbomachinery design models and machine performance calculations. Its effect in nozzle calculation will be illustrated shortly.

Finally, for the \hat{m} calculated using the proposed equation with path-specific λ (dot-dashed lines), the overall agreement with the EOS calculations is very good. Slight deviations are observed in higher Mach number regions with $M > 1$, which cohere to the results observed in Fig. 4. The maximum percentage error in \hat{m} for the proposed equation Eq. (18) is only 0.47%, which is sufficiently accurate for low-order gasdynamic modeling.

2. Analytical solution for isentropic de Laval nozzles

The normalized pressure $\frac{P}{P_0}$ and density $\frac{\rho}{\rho_0}$ from the analytical nozzle solutions were plotted in Fig. 6 using the same legend as Fig. 5. Calculations for three different entropy cases ($s = 1325, 1425,$ and $1525 \text{ JK}^{-1}\text{kg}^{-1}$) are shown on the left, middle and right columns, respectively.

The perfect gas CO_2 calculation still has the greatest error, which originates from the value difference between the actual κ and 1.28 in our study range. The deviation from the EOS calculation reduces with increasing s for the same reason explained in Sec. IV D 1.

Interesting behaviors were found near the throat for results calculated using classic polytropic isentrope equations. A plateau is found for the $s = 1325 \text{ JK}^{-1}\text{kg}^{-1}$ case and a discontinuity was found for $s = 1425$ and $1525 \text{ JK}^{-1}\text{kg}^{-1}$ cases. This is due to the error in the non-dimensional mass flow rate calculation for the classic polytropic assumption that was discussed in Sec. IV D 1. Since the maximum mass flow rate is not at the sonic state $M = 1$ as shown by Fig. 5, the

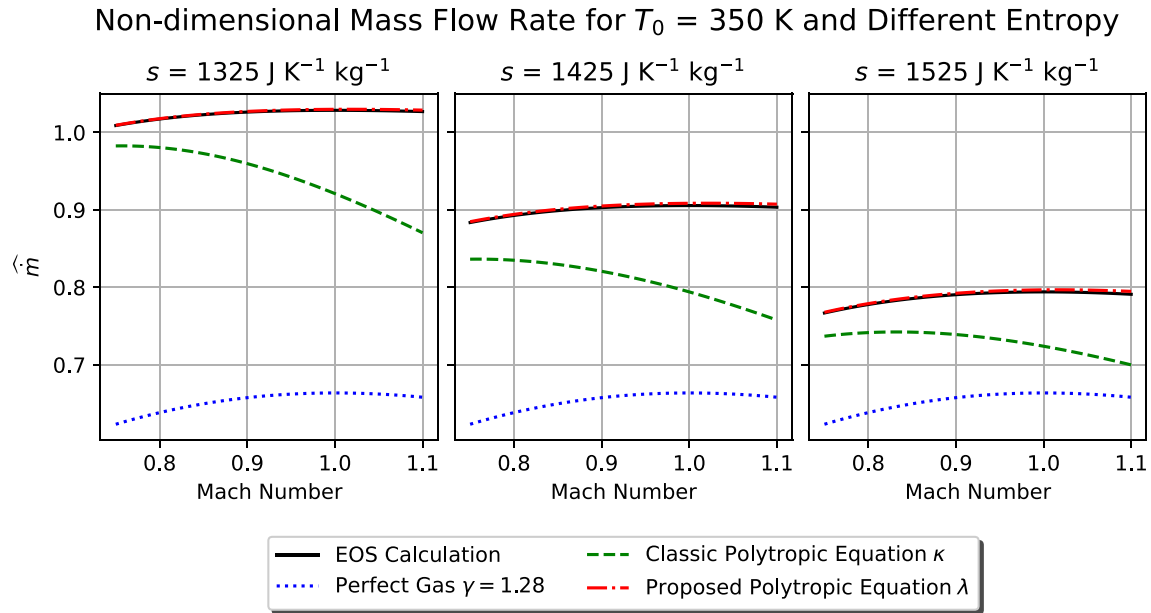


FIG. 5. Non-dimensional mass flow rate comparisons with $T_0 = 350$ K at different entropy levels: $s = 1325, 1425, \text{ and } 1525 \text{ J K}^{-1} \text{ kg}^{-1}$.

choking mass flow rate is underestimated, creating a virtual gap inside the nozzle when solving the continuity equations. Moreover, additional errors from the classic isentropic relations that are up to 50% as shown by Fig. 3 will lead to further deviations from the EOS calculation results.

As for calculation with the new isentropic equation with path-specific λ , the results agree with the EOS analytical solution quite well, indicating a high level of accuracy of the proposed model.

V. CONCLUSION

In conclusion, although equations of state (EOS) can provide accurate calculation of non-ideal fluid isentropic processes, their complexity and implicit nature make them less useful in thermodynamic modeling and design optimization. By contrast, the modified isentropic equation approach offers an alternative with faster explicit expressions. However, it was shown mathematically that the classic polytropic isentropic equation ($Pv^\kappa = \text{Const.}$) is only valid when there is no isentropic expansion coefficient (κ) variation along the isentropes. The direct application of the classic polytropic isentropic equations in non-ideal fluids with large κ variations would lead to significant problems, such as underestimating the choking mass flow rate and inappropriate nozzle designs.

Therefore, to calculate generic non-ideal fluid isentropic processes with κ variations, a new modified polytropic isentropic equation is proposed as $Pv^\lambda = \text{Const.}$ where λ is a path-specific exponent. The polytropic form is preserved in the proposed isentropic equations, allowing the stagnation-to-static property ratio equations to remain in simple form. The explicit nature of the derived equations [Eqs. (16)–(19)] can enable straightforward and rapid calculations of isentropic processes and a better physical understanding. The major contributions and conclusions are as follows:

1. The exponent λ of the proposed polytropic isentropic equation is a path-specific value instead of a state-specific variable κ as the classic isentropic equation, which is widely used in the literature. The difference between λ and κ is to correct for the non-negligible term with $(\frac{\partial \kappa}{\partial v})_s$ in the generic isentropic equation [Eq. (5)]. The difference is more significant with higher Mach numbers and when the static state is near the critical point.
2. The new isentropic relations are derived for pressure [Eq. (16)] and density [Eq. (17)]. Using $s\text{CO}_2$ as an example of non-ideal fluid, the equations' maximum effective relative error (defined in Sec. III B 1) from the exact EOS calculations is below 1.6% while the corresponding classic isentropic relations' [Eqs. (10) and (11)] relative errors are up to 50%. In addition, the results of two other non-ideal fluids, hexamethyldisiloxane (MM) and R-143a, are included to prove the robustness and general applicability of the proposed framework. The proposed method offers greatly simplified expressions for thermodynamics modeling in engineering applications such as turbomachinery reduced-order models and design optimizations.
3. A third-order polynomial with static pressure, density, and Mach number $\lambda(P, \rho, M)$ is provided to calculate λ for $s\text{CO}_2$ within the study range. The maximum effective relative error in the calculated stagnation state is less than 2%, suggesting that the proposed exponent can be well-fitted using simple regression methods. The stagnation states calculation process with the new model and fitted polynomial is around 15 times faster than the exact calculation with EOS.
4. Non-dimensional mass flow rate and analytical nozzle calculations were carried out as test cases to demonstrate the performance of the procedure. The choking mass flow rate can be calculated within 1% from the EOS results using the proposed models while the classic polytropic model can deviate up to 20%

Analytical Nozzle Solution for $T_0 = 420$ K and Different Entropy

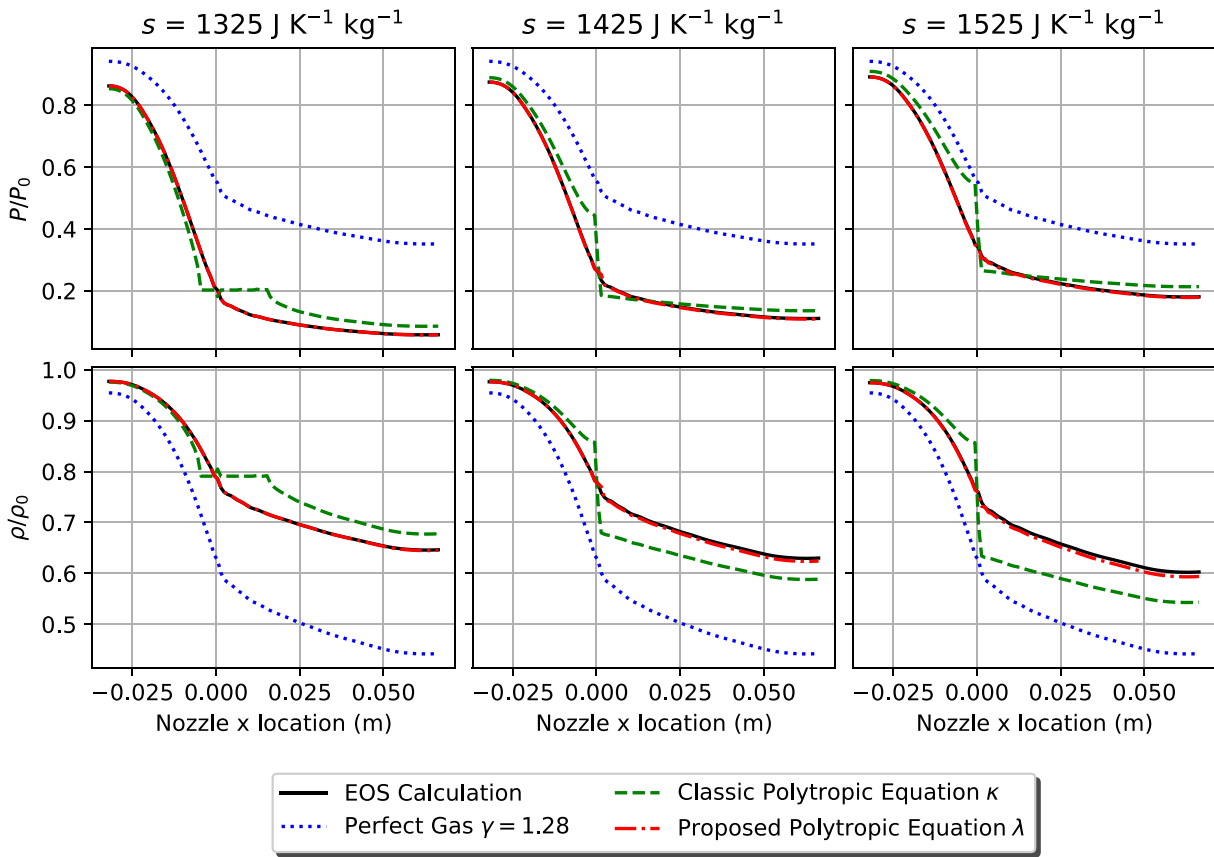


FIG. 6. Analytical nozzle solution for $T_0 = 420$ K at different entropy levels: $s = 1325, 1425, \text{ and } 1525 \text{ JK}^{-1}\text{kg}^{-1}$.

of the EOS calculation. Moreover, the classic polytropic equation failed to predict the maximum mass flow rate at the sonic state, which will lead to nonphysical solutions in de Laval Nozzles. The results show that the proposed model is sufficiently accurate in engineering applications and can hence be used in low-order thermodynamic modeling, such as turbomachinery mean-line models and the evaluation of isentropic efficiencies in thermodynamic cycles.

AUTHOR DECLARATIONS

Conflict of Interest

The authors have no conflicts to disclose.

Author Contributions

Jinhong Wang: Conceptualization (equal); Data curation (lead); Formal analysis (lead); Investigation (lead); Methodology (lead); Validation (lead); Visualization (lead); Writing – original draft (lead); Writing – review & editing (equal). **Teng Cao:** Conceptualization (equal); Formal analysis (supporting); Investigation (supporting); Methodology (supporting); Supervision (lead); Validation

(supporting); Visualization (supporting); Writing – review & editing (equal). **Ricardo Martinez-Botas:** Methodology (supporting); Supervision (supporting); Writing – review & editing (equal).

DATA AVAILABILITY

The data that support the findings of this study are available from the corresponding author upon reasonable request.

NOMENCLATURE

- a_i Polynomial coefficients
- c Speed of sound (m s^{-1})
- c_p Constant pressure heat capacity ($\text{J K}^{-1} \text{kg}^{-1}$)
- c_v Constant volume heat capacity ($\text{J K}^{-1} \text{kg}^{-1}$)
- e Specific internal energy (J kg^{-1})
- h Specific enthalpy (J kg^{-1})
- M Mach number
- m Mass (kg)
- P Pressure (Pa)
- R Specific gas constant ($\text{J K}^{-1} \text{kg}^{-1}$)

- R^2 Coefficient of determinant
- s Specific entropy ($\text{JK}^{-1}\text{kg}^{-1}$)
- T Temperature (K)
- v Specific volume ($\text{m}^3 \text{kg}^{-1}$)
- Z Compressibility factor

Greek letters

- ρ Density (kg m^{-3})
- κ Isentropic expansion coefficient
- λ Proposed path-specific exponent for polytropic isentrope equation
- γ Specific heat capacity ratio

Abbreviations

- AMR Area to Mach number relation
- EOS Equation of state
- RMSE Root mean square error
- sCO₂ Supercritical carbon dioxide
- S-W Span-Wagner
- T-S Temperature-entropy

Subscripts and superscripts

- $\{ \}$ Flow rate (s^{-1})
- $\{ \}_0$ Stagnation state value
- $\{ \}_i$ Different states or locations along a nozzle
- $\hat{\{ \}}$ Non-dimensional form of value Operators
- $\left(\frac{\partial \{ \}}{\partial \{ \}} \right)_X$ Partial differentiation holding property X as constant
- $\text{EOS}_{X_n}(X_a, X_b)$ Equation of state calculation of property X_n using properties X_a and X_b

APPENDIX A: DIFFERENT FORMS OF ISENTROPIC EXPANSION COEFFICIENT

Since the speed of sound is defined as follows:

$$c = \sqrt{\left(\frac{\partial P}{\partial \rho} \right)_s} \tag{A1}$$

The equation of κ can be written in the form of partial derivatives of properties along the isentrope,

$$\kappa = \frac{\rho}{P} \left(\frac{\partial P}{\partial \rho} \right)_s = -\frac{v}{P} \left(\frac{\partial P}{\partial v} \right)_s \tag{A2}$$

Specific heat capacity c_v and c_p are defined as follows:

$$c_v = \left(\frac{\partial e}{\partial T} \right)_v, \quad c_p = \left(\frac{\partial h}{\partial T} \right)_p \tag{A3}$$

From Helmholtz equations, the following can be derived using the triple product rule and Maxwell relations:

$$\begin{aligned} c_v &= T \left(\frac{\partial s}{\partial T} \right)_v \\ &= -T \left(\frac{\partial v}{\partial T} \right)_s \left(\frac{\partial s}{\partial v} \right)_T \\ &= -T \left(\frac{\partial v}{\partial T} \right)_s \left(\frac{\partial P}{\partial T} \right)_v, \end{aligned} \tag{A4}$$

$$\begin{aligned} c_p &= T \left(\frac{\partial s}{\partial T} \right)_p \\ &= -T \left(\frac{\partial P}{\partial T} \right)_s \left(\frac{\partial s}{\partial P} \right)_T \\ &= T \left(\frac{\partial P}{\partial T} \right)_s \left(\frac{\partial v}{\partial T} \right)_p. \end{aligned} \tag{A5}$$

Therefore, with further manipulation using the chain rule and the triple product rule, the heat capacity ratio γ can be derived as follows:

$$\gamma = \frac{c_p}{c_v} = \frac{T \left(\frac{\partial P}{\partial T} \right)_s \left(\frac{\partial v}{\partial T} \right)_p}{-T \left(\frac{\partial v}{\partial T} \right)_s \left(\frac{\partial P}{\partial T} \right)_v} = \frac{\left(\frac{\partial P}{\partial v} \right)_s}{\left(\frac{\partial P}{\partial v} \right)_T}, \tag{A6}$$

and Eq. (A2) can be written as follows:

$$\kappa = -\gamma \frac{v}{P} \left(\frac{\partial P}{\partial v} \right)_T \tag{A7}$$

APPENDIX B: GENERIC ISENTROPE EQUATION DERIVATION

For Eq. (5), Eq. (3) can be rearranged into

$$\frac{\kappa}{v} = -\frac{1}{P} \left(\frac{\partial P}{\partial v} \right)_s \tag{B1}$$

Taking the integral along the isentrope between states 1 and 2 for both sides of the equation,

$$\int_1^2 \frac{\kappa}{v} dv = -\int_1^2 \frac{1}{P} \left(\frac{\partial P}{\partial v} \right)_s dv. \tag{B2}$$

The left-hand side of the equation

$$\int_1^2 \frac{\kappa}{v} dv = \kappa_2 \ln v_2 - \kappa_1 \ln v_1 - \int_1^2 \ln v \left(\frac{\partial \kappa}{\partial v} \right)_s dv. \tag{B3}$$

The right-hand side of the equation can be integrated by parts,

$$-\int_1^2 \frac{1}{P} \left(\frac{\partial P}{\partial v} \right)_s dv = -\ln P_2 + \ln P_1. \tag{B4}$$

Rearranging the left- and right-hand side of the equation,

TABLE III. Dense vapor study range with temperature T in K and entropy s in $\text{JK}^{-1}\text{kg}^{-1}$.

Fluid	T_{crit}	s_{crit}	T_{min}	T_{max}	s_{min}	s_{max}
CO ₂	304.12	1423.41	305	320	1300	1550
MM	518.75	807.39	520	550	700	900
R-143a	345.86	1513.31	346	360	1400	1600

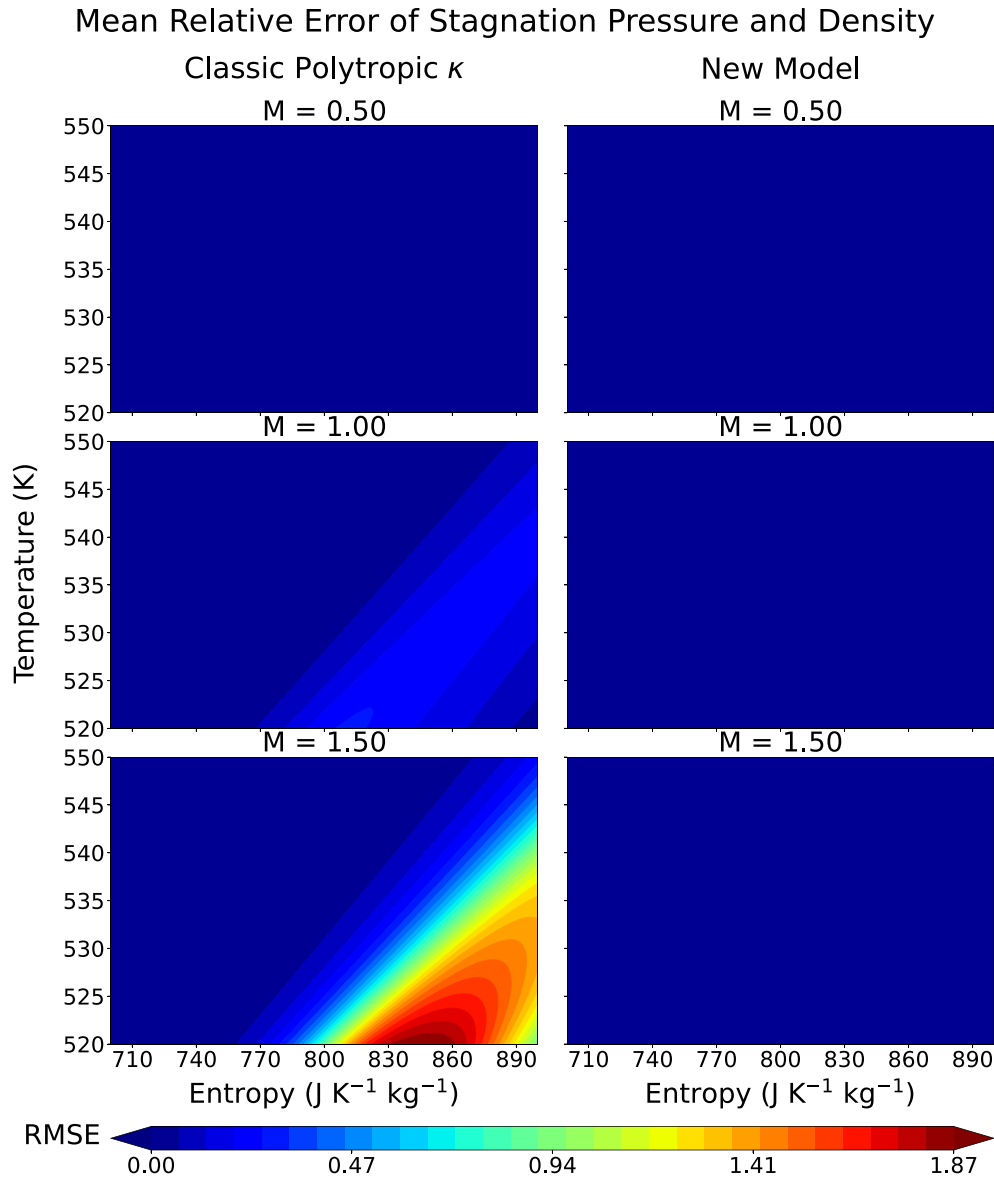


FIG. 7. Effective error comparison between the classic polytropic isentrope equation Eq. (6) (left column) and the new isentrope equation Eq. (14) with optimized λ (right column) at different Mach number for hexamethyldisiloxane (MM).

$$\ln P_1 + \kappa_1 \ln v_1 = \ln P_2 + \kappa_2 \ln v_2 - \int_1^2 \ln v \left(\frac{\partial \kappa}{\partial v} \right)_s dv. \quad (B5)$$

Thus, Eq. (5) can be retrieved,

$$\ln P_1 v_1^{\kappa_1} = \ln P_2 v_2^{\kappa_2} - \int_1^2 \ln v \left(\frac{\partial \kappa}{\partial v} \right)_s dv. \quad (B6)$$

APPENDIX C: NON-DIMENSIONAL MASS FLOW RATE EQUATION DERIVATION

Non-dimensional mass flow rate equation (Eq. (12)) is derived in detail in this section.

First, the mass flow rate equation can be re-written as follows:

$$\begin{aligned} \dot{m} &= \rho UA = \frac{\rho}{\rho_0} \cdot \rho_0 \cdot \frac{U}{c} \cdot c \cdot A = \rho_0 AM \sqrt{\frac{\kappa P}{\rho} \frac{\rho}{\rho_0}} \\ &= \rho_0 AM \sqrt{\kappa} \sqrt{\frac{P}{P_0} \cdot \frac{\rho_0}{\rho} \cdot \frac{P_0}{\rho_0} \frac{\rho}{\rho_0}} \\ &= AM \sqrt{\kappa P_0 \rho_0} \sqrt{\frac{P}{P_0} \frac{\rho}{\rho_0}} \\ &= AM \sqrt{\kappa P_0 \rho_0} \left(1 + \frac{\kappa - 1}{2} M^2 \right)^{-\frac{\kappa + 1}{2(\kappa - 1)}}. \end{aligned} \quad (C1)$$

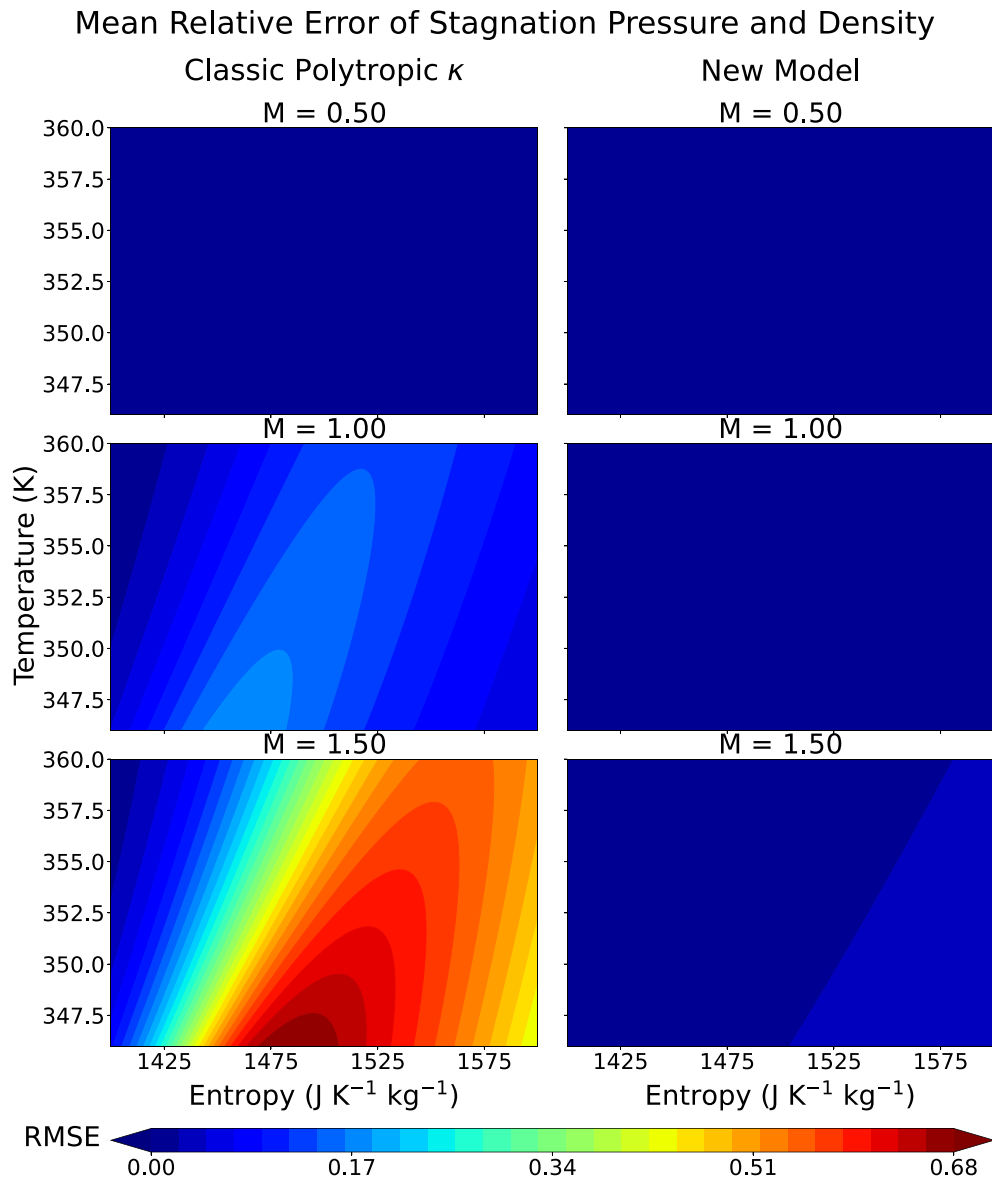


FIG. 8. Effective error comparison between the classic polytropic isentrop equation (6) (left column) and the new isentrop equation (14) with optimized λ (right column) at different Mach number for R-143a.

TABLE IV. Summary of effective errors of classic and proposed polytropic isentrop equations for different non-ideal fluids.

Fluid	Classic polytropic model		Proposed polytropic model	
	RMSE _{avg}	RMSE _{max}	RMSE _{avg}	RMSE _{max}
CO ₂	9.67%	54.44%	0.44%	1.67%
MM	13.65%	187.34%	0.34%	3.87%
R-143a	17.59%	68.42%	0.72%	2.65%

Equations (10) and (11) are used in the last step to simplify the calculation of stagnation-static property ratios.

In Eq. (C1), the non-dimensional values are Mach number M and isentropic expansion coefficient κ ; hence, the non-dimensional mass flow rate \hat{m} can be written as Eq. (12) by rearranging Eq. (C1).

APPENDIX D: VALIDATION WITH OTHER NON-IDEAL FLUIDS

To prove the robustness and general applicability of the proposed models, two additional non-ideal fluids, hexamethyldisiloxane (MM) and R-143a, were used. The corresponding figure with

11 October 2024 09:22:31

TABLE V. Nozzle geometry for nozzle.

Axial coordinate (m)	Normalized area	Axial coordinate (m)	Normalized area
-3.20130×10^{-02}	2.01834	1.81547×10^{-02}	1.03102
-2.90620×10^{-02}	1.98350	2.11057×10^{-02}	1.03566
-2.61109×10^{-02}	1.86624	2.40568×10^{-02}	1.04133
-2.31599×10^{-02}	1.69630	2.70078×10^{-02}	1.04650
-2.02088×10^{-02}	1.52453	2.99588×10^{-02}	1.05202
-1.72578×10^{-02}	1.38187	3.29099×10^{-02}	1.05795
-1.43068×10^{-02}	1.26150	3.58609×10^{-02}	1.06334
-1.13557×10^{-02}	1.16401	3.88120×10^{-02}	1.06832
-8.40468×10^{-03}	1.08926	4.17630×10^{-02}	1.07317
-5.45364×10^{-03}	1.03717	4.47140×10^{-02}	1.07845
-2.50260×10^{-03}	1.00765	4.76651×10^{-02}	1.08384
4.48440×10^{-04}	1.00000	5.06161×10^{-02}	1.08908
3.39948×10^{-03}	1.00547	5.35672×10^{-02}	1.09339
6.35052×10^{-03}	1.00994	5.65182×10^{-02}	1.09627
9.30156×10^{-03}	1.01564	5.94692×10^{-02}	1.09796
1.22526×10^{-02}	1.02050	6.24203×10^{-02}	1.09862
1.52036×10^{-02}	1.02593	6.53713×10^{-02}	1.09824

effective error comparison between the classic polytropic isentrope equation and the proposed isentrope equation like Fig. 3 is included in this section.

The studied ranges of these two dense vapors are included in Table III. Figures 7 and 8 displays the results for MM and R-143a, respectively.

As shown in Figs. 7 and 8, the proposed model is more accurate compared to the classic polytropic isentrope equation. The average and maximum effective errors are summarized in Table IV.

APPENDIX E: NOZZLE GEOMETRY

The nozzle geometry in Table V is a modified version based on the literature.³⁰ The normalized area has been adjusted to ensure that the flow within the nozzle remains fully supercritical at the given stagnation states.

REFERENCES

- D. A. Sullivan, "Historical review of real-fluid isentropic flow models," *J. Fluids Eng.* **103**, 258–267 (1981).
- M. J. Moran, H. N. Shapiro, D. D. Boettner, and M. B. Bailey, *Fundamentals of Engineering Thermodynamics* (John Wiley & Sons, 2010).
- O. Redlich and J. N. S. Kwong, "On the thermodynamics of solutions. V. An equation of state. Fugacities of gaseous solutions," *Chem. Rev.* **44**, 233–243 (1948).
- D.-y. Peng and D. B. Robinson, "A new two-constant equation of state a new two-constant equation of state," *Ind. Eng. Chem. Fundam.* **15**, 59–64 (1976).
- H. K. Onnes, "Expression of the equation of state of gases and liquids by means of series," in *Through Measurement to Knowledge* (Springer, 1991), pp. 146–163.
- R. Span and W. Wagner, "A new equation of state for carbon dioxide covering the fluid region from the triple-point temperature to 1100 K at pressures up to 800 MPa," *J. Phys. Chem. Ref. Data* **25**, 1509–1596 (1996).

- J. W. Strutt, "Aerial plane waves of finite amplitude," *Proc. R. Soc. Lond. A* **84**(570), 247–284 (1910).
- H. L. Callendar, "On the thermodynamical properties of gases and vapours as deduced from a modified form of the Joule–Thomson equation, with special reference to the properties of steam," *Proc. R. Soc. London* **67**, 266–286 (1901).
- W. J. Walker, "CXXXIV. Specific heat variations in relation to the dynamic action of gases and their equations of state," *London, Edinburgh, Dublin Philos. Mag. J. Sci.* **50**, 1244–1260 (1925).
- E. W. Lemmon, I. H. Bell, M. L. Huber, and M. O. McLinden, "NIST Standard Reference Database 23: NIST reference fluid thermodynamic and transport properties database (REFPROP)," Version 10.0, Standard reference data, National Institute of Standards and Technology, Gaithersburg, MD, 2018, pp. 288–290.
- J. Wang, T. Cao, and R. Martinez-Botas, "Supercritical carbon dioxide shock behavior near the critical point," *J. Eng. Gas Turbines Power* **146**, 011010 (2024).
- P. Nesterstigt and R. Pecnik, "Generalised isentropic relations in thermodynamics," *Energies* **16**, 2281 (2023).
- Y. Wang and J. Yan, "Study of performance changes in centrifugal compressors working in different refrigerants," *Energies* **17**, 2784 (2024).
- D. Baumgärtner, J. J. Otter, and A. P. Wheeler, "The effect of isentropic exponent on transonic turbine performance," *J. Turbomach.* **142**, 081007 (2020).
- N. D. Baltadjiev, "An investigation of real gas effects in supercritical CO₂ compressors," Ph.D. thesis, Massachusetts Institute of Technology, 2012.
- N. D. Baltadjiev, C. Lettieri, and Z. S. Spakovszky, "An investigation of real gas effects in supercritical CO₂ centrifugal compressors," *J. Turbomach.* **137**, 091003 (2015).
- D. A. Kouremenos and X. K. Kakatsios, "The three isentropic exponents of dry steam," *Forsch. Ingenieurwes.* **51**, 117–122 (1985).
- F. Tosto, C. Lettieri, M. Pini, and P. Colonna, "Dense-vapor effects in compressible internal flows," *Phys. Fluids* **33**, 086110 (2021).
- A. S. Iberall, "The effective "gamma" for isentropic expansions of real gases," *J. Appl. Phys.* **19**, 997–999 (1948).
- T. Jia, P. Dou, P. Chu, Y. Dai, and C. N. Markides, "Development and performance evaluation of a high solar contribution resorption-compression cascade heat pump for cold climates," *Energy* **302**, 131806 (2024).
- D. A. Kouremenos and K. A. Antonopoulos, "Isentropic exponents of real gases and application for the air at temperatures from 150 K to 450 K," *Acta Mech.* **65**, 81–99 (1987).
- D. A. Kouremenos and K. A. Antonopoulos, "Sound velocity and isentropic exponents for gases with different acentric factors by using the Redlich–Kwong–Soave equation of state," *Acta Mech.* **66**, 177–189 (1987).
- G. H. Schnerr and P. Leidner, "Diabatic supersonic flows of dense gases," *Phys. Fluids A* **3**, 2445–2458 (1991).
- I. H. Bell, J. Wronski, S. Quoilin, and V. Lemort, "Pure and pseudo-pure fluid thermophysical property evaluation and the open-source thermophysical property library CoolProp," *Ind. Eng. Chem. Res.* **53**, 2498–2508 (2014).
- N. Diepstraten, L. M. Somers, and J. A. van Oijen, "Numerical characterization of high-pressure hydrogen jets for compression–ignition engines applying real gas thermodynamics," *Int. J. Hydrogen Energy* **79**, 22–35 (2024).
- S. A. Wright, R. F. Radel, M. E. Vernon, G. E. Rochau, and P. S. Pickard, "Operation and analysis of a supercritical CO₂ Brayton cycle," SANDIA Report SAND2010-0171, Sandia National Laboratories, 2010, pp. 1–101.
- P. Cinnella, P. M. Congedo, and D. Laforgia, "Transonic flows of BZT fluids through turbine cascades," *Comput. Fluid Dyn.* **2004**, 227–232 (2006).
- D. A. Kouremenos and X. K. Kakatsios, "Ideal gas relations for the description of the real gas isentropic changes," *Forsch. Ingenieurwes.* **51**, 169–174 (1985).
- P. Virtanen, R. Gommers, T. E. Oliphant, M. Haberland, T. Reddy, D. Cournapeau, E. Burovski, P. Peterson, W. Weckesser, J. Bright, S. J. van der Walt, M. Brett, J. Wilson, K. J. Millman, N. Mayorov, A. R. J. Nelson, E. Jones, R. Kern, E. Larson, C. J. Carey, I. Polat, Y. Feng, E. W. Moore, J. VanderPlas, D. Laxalde, J. Perktold, R. Cimrman, I. Henriksen, E. A. Quintero, C. R. Harris, A. M. Archibald, A. H. Ribeiro, F. Pedregosa, and P. van Mulbregt, "SciPy 1.0: Fundamental algorithms for scientific computing in python," *Nat. Methods* **17**, 261–272 (2020).
- C. Lettieri, D. Paxson, Z. Spakovszky, and P. Bryanston-Cross, "Characterization of nonequilibrium condensation of supercritical carbon dioxide in a de Laval Nozzle," *J. Eng. Gas Turbines Power* **140**, 041701 (2018).